

Strangeness Content in the Nucleon

Keh-Fei Liu ‡

Department of Physics, University of Kentucky, Lexington, KY 40506, USA

Abstract. I will review recent studies of strangeness content in the nucleon pertaining to the flavor-singlet g_A^0 , the $\bar{s}s$ matrix element and the strangeness electric and magnetic form factors $G_E^s(q^2)$ and $G_M^s(q^2)$, based on lattice QCD calculations. I shall also discuss the relevance of incorporating the strangeness content in nuclei in regard to strange baryon-antibaryon productions from proton-nucleus and nucleus-nucleus collisions at SPS and RHIC energies.

1. Introduction

There has been a great deal of interest of late in measuring and understanding the strangeness content of the nucleon. This includes the strangeness magnetic moment [1, 2] and electric form factor [3], the $\bar{s}s$ matrix element and $\pi N\sigma$ term [4], the strange quark polarization [5] and orbital angular momentum [6], and the strange to non-strange sea ratio in deep inelastic scattering [7]. Why do we concern ourselves with strangeness in the nucleon at all? Why is there a surge of interest in this subject recently? Is it relevant to the production of strange and anti-strange hadrons in proton-nucleus and nucleus-nucleons collisions at relativistic energies which, of course, is the focus of this conference? These are the issues that I want to discuss in this talk.

The conventional wisdom based on the valence quark model picture suggests that there is no need to consider strangeness in the nucleon. This is so because valence quark models have been successful in describing hadron spectroscopy [8, 9, 10, 11] and baryon magnetic moments [8, 12, 13], especially the neutron to proton magnetic moment ratio μ_n/μ_p . It is also successful in delineating the pattern of electromagnetic [14, 15, 16], semileptonic and nonleptonic weak decays [17]. In particular, up until late eighties, there had not been a prevailing reason to question the validity of the Okubo-Zweig-Iizuka (OZI) rule [18] which seemed to work well in the available experiments. Thus, there is no compelling reason to include the higher Fock space such as $s\bar{s}$ pair in the nucleon wavefunction beyond the valence u and d quarks.

On the other hand, there have been hints all along that the valence quark model for the light hadrons is incomplete and inadequate in elucidating a number of quantities and relations. Examples abound, they include the η' meson mass – the $U(1)$ anomaly, the vector dominance, the Goldberger-Treiman relation and the $\pi N\sigma$ term puzzle. These examples can be understood in terms of sea quarks and meson clouds via models and current algebra based on chiral symmetry, an inherent symmetry in QCD. However, these warnings did not amount to a wake up call about the shortcomings of

‡ liu@pa.uky.edu

Invited talk presented at V International Conference on Strangeness in Quark Matter, “Strangeness 2000”, Berkeley, CA, July 20–25, 2000

the valence quark model until the discovery of the large and negative polarization of the strange quark in polarized deep inelastic scattering [19, 20, 21] which led to a small flavor-singlet g_A^0 , about $\frac{1}{4}/\frac{1}{3}$ of that predicted by the non-relativistic/relativistic quark model. This discrepancy has not been satisfactorily explained in any hadronic model and has been dubbed the ‘proton spin crisis’. It is mostly understood only through direct calculations in lattice QCD [22, 23, 24]. This, I believe, is a watershed in hadron physics. From this point on, people are forced to take the intrinsic strangeness, and sea quarks for that matter, in the nucleon seriously.

I shall illustrate the role of strangeness in three examples, namely the flavor-singlet g_A^0 , the $\langle N|\bar{s}s|N\rangle$ matrix element, and the strangeness magnetic moment and electric form factor. I shall mainly discuss what we have learned from the available lattice QCD calculations. Lattice QCD offers an *ab initio* method of computing the non-perturbative properties of the strong interaction; it can account for all characteristics of nucleon and hadron properties to arbitrary accuracy, in principle. In practice, it is subject to great technical challenges which however are being addressed with increasingly sophisticated computational, algorithmic and theoretical ideas [25]. An important goal has been to make a quantitative test of QCD — to demonstrate that the underlying dynamics of quarks and gluons, as specified by QCD, can describe accurately the properties, as observed in the laboratory, of nucleons and other hadrons. This has not been achieved yet, but as numerical simulations of increasing size and sophistication are applied to this problem, we see QCD being able to account with increasing detail for the structure of the hadronic world.

For the short term, it proves to be beneficial to carry out quenched lattice calculations to gain qualitative and semi-quantitative understanding on the physical quantities that are not reliably obtainable from the present models. Model predictions on these quantities can differ by as much as a factor of 3 to 5 (e.g. the monopole mass in the πNN form factor, the strangeness content $\bar{s}s$ in the nucleon, and the $E2/M1$ ratio in $N\gamma \leftrightarrow \Delta$) and sometimes differ even in sign (e.g. the strange magnetic moment and electric form factor in the nucleon). Even though our present lattice calculation based on the Wilson fermion in the quenched approximation may have a systematic error as large as 20% for the connected insertion (valence and connected sea) part and maybe larger for the disconnected insertion (disconnected sea) part, it is already better than the systematic errors spanned by the model dependence. Furthermore, the systematic errors of these quantities can be put under control when the study of the large volume, continuum limit, and chiral limit are included. These systematic errors will be addressed with Neuberger’s overlap fermion [26] which has lattice chiral symmetry and good scaling behavior. In addition, it admits numerical calculation close to the physical quark masses (e.g. physical pion mass at 200 MeV) without significant critical slowing down [27]. Systematic errors due to the dynamical fermion effect will have to be addressed when enough computer resources are available. The present day dynamical fermion simulations are still performed with quite heavy quarks which may not reflect the realistic quark loop effects beyond a shift in coupling constant like a dielectric constant effect [28].

2. Strangeness Content in the Nucleon

2.1. Flavor-singlet g_A^0 – Quark Spin Content of the Nucleon

The polarized DIS experiments [19, 20, 21] found a surprisingly small flavor-singlet axial coupling constant g_A^0 (0.27(10) [20] and 0.28(16) [21]). Being the quark spin content of the nucleon; i.e. $g_A^0 = \Delta u + \Delta d + \Delta s$, this is much smaller than the expected value of unity from the non-relativistic quark model or 0.75 from the $SU(6)$ relation (i.e. $3/5$ of the isovector coupling $g_A^3 = 1.2574$). This has attracted a lot of theoretical attention [29] and the ensuing confusion was dubbed the “proton spin crisis”.

Direct lattice calculations of g_A^0 from the forward matrix element of the flavor-singlet axial current has been carried out and the smallness of g_A^0 is understood [22, 23, 24]. As a flavor-singlet quantity, g_A^0 is composed of two components. One is from the connected insertion (C.I.) and the other is from the disconnected insertion (D.I.). Therefore, $g_A^0 = g_A^0(C.I.) + g_A^0(D.I.)$ where $g_A^0(C.I.)$ is obtained from the connected insertion in Fig. 1(a) and $g_A^0(D.I.)$ is obtained from the disconnected insertion in Fig. 1(b). Lattice calculation [22] indicates that each of the $u, d,$ and s flavors contributes -0.12 ± 0.01 to the D.I. (Fig. 1(b)). This negative vacuum polarization from the disconnected sea quarks is largely responsible for bringing the value of g_A^0 from $g_A^0(C.I.) = 0.62 \pm 0.09$ to 0.25 ± 0.12 , in agreement with the experimental value (See Table 1). This is an example where the disconnected sea contributes substantially and leads to a large breaking in the $SU(6)$ relation. Thus, it is understandable that it should come as a surprise to the valence quark model — the latter does not have the sea degree of freedom, disconnected or connected, and has simply ignored it by assuming the OZI rule.

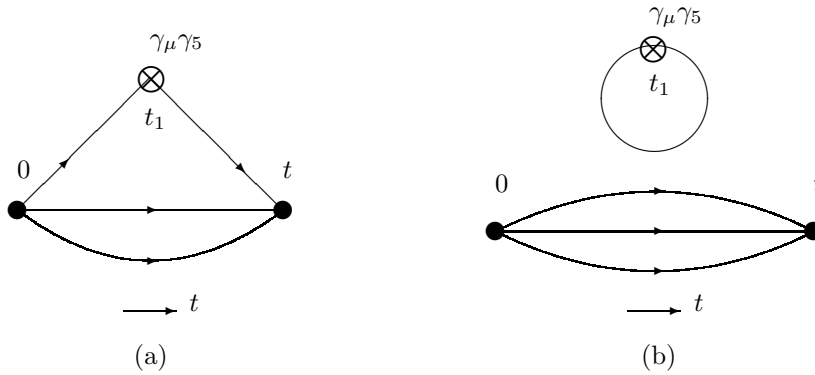


Figure 1. Quark line diagrams of the three-point function in the Euclidean path integral formalism for evaluating g_A^0 from the flavor-singlet axial-vector current. (a) is the connected insertion which contains the valence and connected sea degrees of freedom and (b) is the disconnected insertion which contains the disconnected quark sea.

We see in Table 1 that the calculated result of the strange polarization Δs is in

Table 1. Axial coupling constants and quark spin contents of proton in comparison with experiments, the non-relativistic quark model (NRQM), and the relativistic quark model (RQM).

	C. I.	C. I. + D. I.	Experiments	NRQM	RQM
$g_A^0=\Delta u+\Delta d+\Delta s$	0.62(9)	0.25(12)	0.28(16) [21], 0.27(10)[20]	1	0.754
$g_A^3=\Delta u-\Delta d$	1.20(10) [30]	1.20(10)	1.2573(28)	5/3	1.257
$g_A^8=\Delta u+\Delta d-2\Delta s$	0.62(9)	0.61(13)	0.579(25) [33]	1	0.754
Δu	0.91(10)	0.79(11)	0.82(5)[21], 0.82(6)[20]	4/3	1.01
Δd	-0.29(10)	-0.42(11)	-0.44(5)[21], -0.44(6) [20]	-1/3	-0.251
Δs		-0.12(1)	-0.10(5)[21], -0.10(4) [20]	0	0
$F_{A=(\Delta u-\Delta s)/2}$	0.45(6)	0.45(6)	0.459(8) [33]	2/3	0.503
$D_{A=(\Delta u-2\Delta d+\Delta s)/2}$	0.75(11)	0.75(11)	0.798(8) [33]	1	0.754
F_A/D_A	0.60(2)	0.60(2)	0.575(16) [33]	2/3	2/3

good agreement with the experiments. Since the contribution from the strange quark comes only from the disconnected sea in Fig. 1(b) [31], the role of the strange and the disconnected sea contribution from u and d quarks is clear and well-defined in the three-point function as illustrated in Fig. 1(b). From the path-integral formulation of the hadronic tensor, it is learned [31, 32] that there is connected sea in the form of the non-perturbative Z -graphs in the C.I. represented by Fig. 1(a) which is responsible for the violation of the Gottfried sum rule, for example. Although the strange quark does not contribute to the connected sea in Fig. 1(b), it is still interesting to find out what effect the connected sea has on the physical quantities we are studying. Since the connected sea contribution to the C.I. of three-point functions is entangled with the valence, we can not separate it out as is done for the disconnected sea. To see its effect indirectly, we consider the ratio

$$\begin{aligned}
 R_A &= \frac{g_A^0}{g_A^3} = \frac{\Delta u + \Delta d + \Delta s}{\Delta u - \Delta d} \\
 &= \frac{(\Delta u + \Delta d)(C.I.) + (\Delta u + \Delta d + \Delta s)(D.I.)}{\Delta u - \Delta d}
 \end{aligned} \tag{1}$$

as a function of the quark mass. Our results which correspond to the range between strange and twice the charm masses are plotted in Fig. 2 as a function of the quark mass $ma = \ln(4\kappa_c/\kappa - 3)$. The dotted line is the valence quark model prediction of 3/5 for both the non-relativistic and relativistic cases. For heavy quarks (i.e. $\kappa \geq 0.133$ or $ma \geq 0.4$ in Fig. 2), we see that the ratio R_A is 3/5 irrespective of whether the D.I. is included (shown as \bullet in Fig. 2) or not (C.I. alone is indicated as \circ). This is to be expected because the disconnected/connected sea quarks which are pair produced via the Z -graphs/loops are suppressed for non-relativistic quarks by $O(p/m_q)$ or $O(v/c)$. As for light quarks, the full result (C.I. + D.I.) is much smaller than 3/5 largely due to the negatively polarized sea contribution in the D.I. (NB. Table 1 lists the results at the chiral limit.) Even for the C.I. alone, R_A still dips under 3/5. As we shall see later this is caused by the disconnected sea quarks.

Now, we turn to valence QCD [32]. This is the case where the quark is forbidden to propagate backward in time so that there is no pair creation and, as a result, only the valence u and d quarks are present in a ‘nucleon’. The motivation of studying this mutilated QCD is to establish a connection between QCD and the valence quark model [32]. The same 100 gauge configurations used for quenched QCD calculation

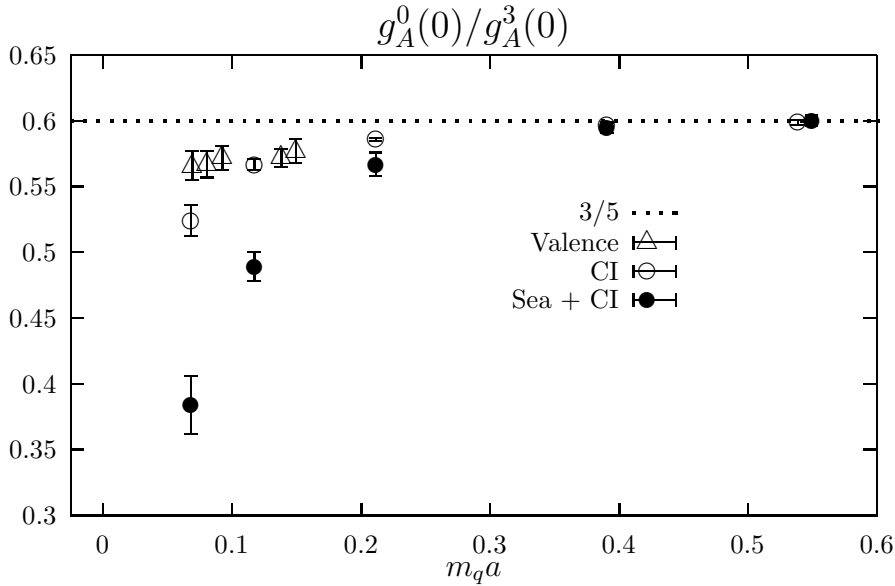


Figure 2. The ratio R_A between isoscalar and isovector g_A in VQCD and QCD are plotted against the dimensionless quark mass $m_q a$ from the strange to the charm region. \triangle indicates the VQCD case, \circ/\bullet indicates the C.I./ D.I. + C.I. in the QCD case. The dashed line is the $SU(6)$ prediction of $3/5$.

are used for the valence QCD (VQCD) case. Since in VQCD there is only C.I. (Fig. 1(a)), the R_A ratio in Eq. (1) becomes

$$R_A = \frac{g_A^0}{g_A^3}(C.I.) = \frac{(\Delta u + \Delta d)(C.I.)}{(\Delta u - \Delta d)(C.I.)}. \quad (2)$$

The results are plotted in Fig. 2 as a function of the dimensionless quark mass $m_q a$ (with $\kappa = 0.162, 0.1615, 0.1610, 0.1590,$ and 0.1585) in comparison with the QCD case. We see that, even for light quarks in the strange region ($m_q a \sim 0.07$), it is much closer to the valence prediction of $3/5$, in contrast to the QCD calculation with C.I. alone. This shows that VQCD indeed seems to confirm our expectation of the valence quarks behavior, i.e. obeying the $SU(6)$ relation. The deviation from the exact $3/5$ prediction in Fig. 2 reflects the fact that there is still a spin-spin interaction between the valence quarks as evidenced in the $\vec{\sigma} \cdot \vec{B}$ term in the VQCD action with Pauli spinors [32]. Its effect, however, appears to be small. This also confirms our earlier assertion that the deviation of the C.I. of R_A in QCD (\circ in Fig. 2) is largely due to the the connected sea quark-antiquark pairs.

With only the C.I., the F_A/D_A ratio is related to VQCD R_A in Eq. (2)

$$\frac{F_A}{D_A}(C.I.) = \frac{1 + R_A}{3 - R_A}, \quad (3)$$

From $R_A = 0.566(11)$ for the smallest quark mass ($\kappa = 0.162$), we obtain $F_A/D_A = 0.643(4)$. The fact that this is only slightly larger than the QCD prediction of $0.60(2)$ for the C.I. (see Table 1) has to do with the fact that the disconnected sea contribution is essentially independent of flavor in our calculation, i.e. $\Delta u_s = \Delta d_s = \Delta s$ [22]. As a result, F_A , D_A , and the F_A/D_A ratio are identical with or without the sea quarks

from the D.I. (see Table 1) and they do not reflect the large disconnected sea effect due to the individual flavor.

2.2. Scalar Matrix Elements, R_S , and D_S/F_S

Similar situation exists for the scalar current matrix elements. It has been suggested that the well-known $\pi N\sigma$ term ($\sigma_{\pi N} = \hat{m}\langle N|\bar{u}u + \bar{d}d|N\rangle$ with $\hat{m} = (m_u + m_d)/2$) puzzle [34, 35] can be resolved because of the large OZI violating contribution from the sea with a large $\bar{s}s$ content in the nucleon [34, 36] such that $y = 2\langle N|\bar{s}s|N\rangle/\langle N|\bar{u}u + \bar{d}d|N\rangle \sim 0.2 - 0.3$. This has been verified in lattice calculations [37, 38, 39] which show that the D.I. is ~ 1.8 times of the C.I. (see Table 2) [38] and the y ratio as large as 0.36 ± 0.03 [38].

Table 2. Scalar contents, $\sigma_{\pi N}$, F_S , and D_S , in comparison with phenomenology and quark model (QM). The 17.7 MeV in the last column is determined with the quark mass from the lattice calculation.

	C. I.	C.I + D.I.	Phenomenology	QM
$\langle p \bar{u}u + \bar{d}d p\rangle$	3.02(9)	8.43(24)		≤ 3
$\langle p \bar{u}u - \bar{d}d p\rangle$	0.63(9)			≤ 1
$\langle N \bar{s}s N\rangle$	1.53(7)			0
F_S	0.91(13)	1.51(12)	1.52 [40, 41] — 1.81[42]	≤ 1
D_S	-0.28(10)	-0.88(28)	-0.52[40, 41] — -0.57[42]	0
$\sigma_{\pi N}$	17.8(5) MeV	49.7(2.6) MeV	45 MeV [35]	≤ 17.7 MeV

Unlike the case of the axial current matrix element, different flavors contribute differently to the D.I. of the scalar matrix element – s contributes less than u and d . As a result, the $SU(3)$ antisymmetric and symmetric parameters, $F_S = (\langle p|\bar{u}u|p\rangle - \langle N|\bar{s}s|N\rangle)/2$, $D_S = (\langle p|\bar{u}u|p\rangle - 2\langle p|\bar{d}d|p\rangle + \langle N|\bar{s}s|N\rangle)/2$ are strongly affected by the large D.I. part. We see from Table 2 that both D_S and F_S compare favorably with the phenomenological values obtained from the $SU(3)$ breaking pattern of the octet baryon masses with either linear [40, 41] or quadratic mass relations [42]. This agreement is significantly improved from the valence quark model which predicts $F_S < 1$ and $D_S = 0$ and also those of the C.I. alone [40, 41]. The latter yields $F_S = 0.91(13)$ and $D_S = -0.28(10)$ which are only half of the phenomenological values [40, 41, 42]. This again underscores the importance of the disconnected sea-quark contributions.

Next, we address the effect of the connected sea quarks in the C.I.. Similar to the ratio R_A in the axial-vector case, we plot the ratio

$$\begin{aligned}
 R_S &= \frac{g_S^{I=0}}{g_S^{I=1}} = \frac{\langle p|\bar{u}u + \bar{d}d|p\rangle}{\langle p|\bar{u}u - \bar{d}d|p\rangle} \\
 &= \frac{(\langle p|\bar{u}u + \bar{d}d|p\rangle)(C.I.) + (\langle p|\bar{u}u + \bar{d}d|p\rangle)(D.I.)}{\langle p|\bar{u}u - \bar{d}d|p\rangle} \quad (4)
 \end{aligned}$$

as a function of the quark mass in Fig. 3.

The dotted line is the valence quark model prediction of 3 for both the non-relativistic and relativistic cases. Again for heavy quarks (i.e. $\kappa \geq 0.133$ or $ma \geq 0.4$ in Fig. 3), we see that the ratio R_S is 3 irrespective whether the D.I. is included (shown as \bullet in Fig. 3) or not (C.I. alone is indicated as \circ). As for light quarks, the full result (C.I. + D.I.) is much larger than 3 largely due to the large contribution in

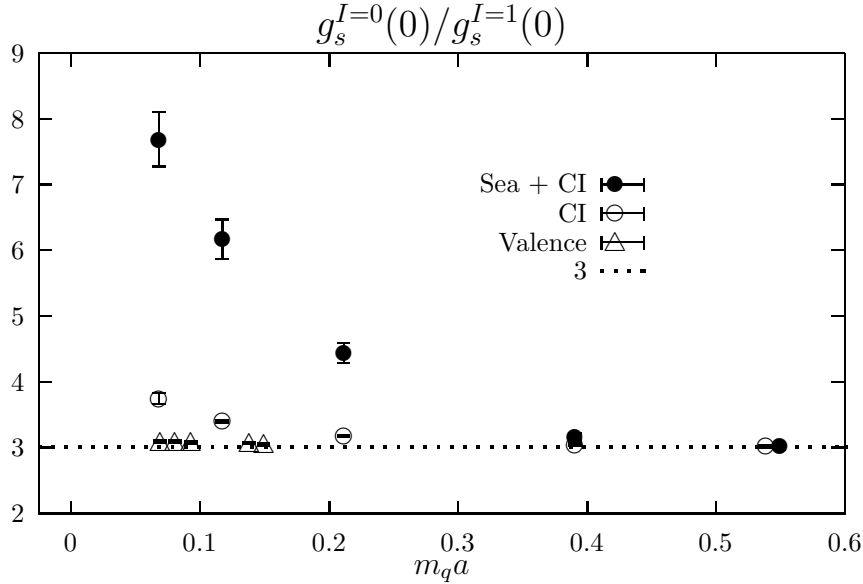


Figure 3. The ratio R_S between isoscalar and isovector scalar charge in QCD (Eq. (4)) and VQCD (Eq. (5)) are plotted against the dimensionless quark mass $m_q a$ from the strange to the charm region. \circ/\bullet indicates the C.I./ D.I. + C.I. in the QCD case and \triangle indicates the VQCD case. The dashed line is the valence quark model prediction of 3.

the D.I. (NB. Table 2 lists the results at the chiral limit). Even for the C.I. alone, R_S still overshoots 3. As we shall see, this is again caused by the connected sea quarks. For VQCD, the R_S ratio becomes

$$R_S = \frac{(\langle p | \bar{u}u + \bar{d}d | p \rangle)(C.I.)}{(\langle p | \bar{u}u - \bar{d}d | p \rangle)(C.I.)}. \quad (5)$$

We see in Fig. 3 that the ratios (denoted by \triangle) for the light quarks are approaching the valence quark prediction of 3. This again confirms that the deviation of the C.I. result in QCD is primarily due to the Z -graphs with connected sea quarks and antiquarks. When they are eliminated in VQCD, R_S becomes close to the $SU(6)$ relation.

The D_S/F_S ratio in VQCD is

$$D_S/F_S(C.I.) = \frac{3 - R_S}{1 + R_S}, \quad (6)$$

From $R_S = 3.086(19)$ for the smallest quark mass ($\kappa = 0.162$), we obtain $D_S/F_S = -0.021(4)$ which is close to zero as in the valence quark picture (Table 2) and differs from the lattice QCD calculation of $-0.58(18)$ (D.I. + C.I.) and $-0.31(11)$ (C.I.) (see Table 2) by a large margin.

2.3. Strangeness Magnetic Moment and Neutron to Proton Magnetic Moment Ratio

After having established the importance of the strangeness sea effects in the axial and scalar matrix elements, one would naturally ask what happens to the vector current matrix elements, especially the neutron to proton magnetic moment ratio μ_n/μ_p . How much will the sea affect the ratio and in what way? After all, the μ_n/μ_p ratio was

well predicted by the valence picture – a celebrated defining success of the $SU(6)$ symmetry.

The strangeness contribution to the proton electric and magnetic form factors $G_E^s(q^2)$ and $G_M^s(q^2)$ can be extracted from parity violating asymmetry measured in the polarized electron proton scattering [1]. The first result coming out of the SAMPLE experiment [43] gives the strangeness magnetic form factor $G_M^s(Q^2 = 0.1\text{GeV}^2) = 0.23 \pm 0.37 \pm 0.15 \pm 0.19$ n.m. Combined with data from the deuteron, the new result is closer to zero with a relatively larger error [1]. Our lattice analysis gives $G_M^s(Q^2 = 0) = -0.36 \pm 0.20$ n.m. [44]. With an unbiased subtraction to reduce the noise, the new analysis gives $G_M^s(Q^2 = 0) = -0.28 \pm 0.10$ n.m. [45]. Although it is consistent with the SAMPLE experiment within error bars, the central value may differ by a sign. Theoretically, very little is known about the strangeness contribution to the EM form factor of the nucleon. Even the sign of the strangeness contribution to the magnetic moments is uncertain. Different model gives different prediction, including its sign [46]. Hopefully, the experimental results will be clearer when the approved experiments at CEBAF (Hall C experiment 91-017) [3] start to produce results. We have also calculated the strange electric form factor $G_E^s(q^2)$ and found it to be small and positive. This is going to be a prediction which can be checked by the CEBAF experiments [3].

According to the lattice calculation [44], the u and d contributions are $\sim 80\%$ larger, $G_M^{u,d}(0)(D.I.) = -0.65 \pm 0.30$. However, their net contribution to the proton and neutron magnetic moment

$$\begin{aligned} \mu(D.I.) &= (2/3G_M^u(0)(D.I.) - 1/3G_M^d(0)(D.I.) - 1/3G_M^s(0))\mu_N \\ &= -0.097 \pm 0.037\mu_N \end{aligned} \quad (7)$$

becomes smaller due the cancellation of the quark charges of u , d , and s . The result still holds within error after the unbiased subtraction [45].

As illustrated in Fig. 4, where the neutron to proton magnetic moment ratio is plotted against the quark mass, this small $SU(6)$ -breaking sea quark effect is further nullified by the connected sea effect [44]. As a result, the μ_n/μ_p ratio for the combined C.I. and D.I. comes to -0.68 ± 0.04 at the chiral limit. This is quite consistent with the experimental value of -0.685 . Barring any as yet unknown symmetry principle, this cancellation between the connected and disconnected sea contributions is probably accidental and in stark contrast to the $\pi N\sigma$ term and flavor-singlet g_A^0 where the connected and disconnected sea effects add up to enhance the $SU(6)$ breaking.

Also shown in Fig. 4 are results of VQCD (indicated as Δ) which are very close to the $SU(6)$ value of $-2/3$ (the result for the smallest quark mass case is $-0.662(22)$), indirectly verifying the connected sea effect of QCD (\circ for the C.I. in Fig. 4) which shows a 2.5σ departure from $-2/3$ at the chiral limit. If there is any deviation of the VQCD from $-2/3$, it should be due to the residual spin-spin interaction between the quarks in the baryon. Given the size of the error in our present results, we cannot make a definite conclusion on this aspect.

3. Hyperon-Antihyperon Production in Nucleus-Nucleus Collisions

We see from the previous section that there are large strangeness contents in the nucleon. The strangeness quark spin ($\Delta s = -0.12(1)$) is 12% of the total nucleon

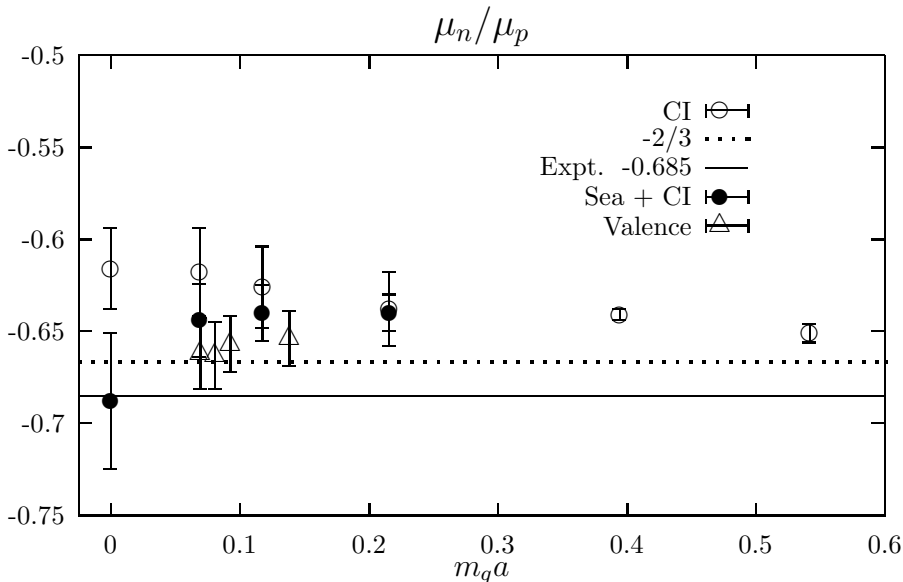


Figure 4. The ratio of neutron to proton magnetic moment μ_n/μ_p is plotted against the dimensionless quark mass. \circ indicates the C.I. result only and \bullet shows the full result with both C.I. and D.I. and \triangle indicates the ratio in the VQCD case. The solid line is the valence quark model prediction of $-2/3$ and the dashed line is the experimental result of -0.685 .

angular momentum, albeit in the opposite direction. The scalar matrix element for the strange is also large. With the ratio $\langle N|\bar{s}s|N\rangle/\langle N|\bar{u}u + \bar{d}d|N\rangle = 0.18 \pm 0.02$ from the lattice calculation, the strangeness accounts for $\sim 18\%$ of the nucleon content in the scalar channel. This strongly suggests that one needs to take the $s\bar{s}$ content in the form of $\bar{s}s, \bar{s}\gamma_\mu\gamma_5 s, \bar{s}\gamma_\mu s, \bar{s}\gamma_5 s$, etc. in the nucleon wavefunction in addition to the valence u and d quark wavefunction.

We heard in this conference [47] that various experiments at CERN SPS revealed an enhancement of strange particle production from proton-proton and proton-nucleus to nucleus-nucleus collision [48, 49]. Upon analyzing their Pb-Pb data and comparing to p-Be and p-Pb data, the WA97 collaboration found an enhancement in hyper-antihyperon ($\Lambda, \bar{\Lambda}, \Xi^-, \bar{\Xi}^+, \Omega^-, \bar{\Omega}^+$) yields per participant nucleon (wounded nucleon participating in the collisions as estimated from the Glauber model) [48]. Furthermore, the enhancement is shown to increase with the valence strangeness in the produced hyperon (antihyperon) [48]. Besides the scenario of equilibrated quark gluon plasma phase [50, 51], several mechanisms have been considered theoretically in view of this enhancement. They include the baryon junction exchange mechanism [52], the diquark breaking mechanism [53], and the strong color field effect [54].

In view of the existence of non-negligible strangeness content in the nucleon, it seems to me that one should take it into account in the hyperon-antihyperon production from the proton-nucleus and nucleus-nucleus collisions at high energies. Since the sea-quark content is relatively small compared to the valence, it should be a good approximation to consider one pair of $u\bar{u}, d\bar{d}$ and $s\bar{s}$ in the higher Fock space. In this case, we can point out a difference between the p-nucleus and nucleus-nucleus collisions. In the p-nucleus collision, the $\Omega^- - \bar{\Omega}^+$ production can only come from the

pair-creation via perturbative gluons which is characterized by the coupling constant α_s at the SPS energy or string breaking. On the other hand, the nucleus-nucleus collision can involve additional mechanisms. For example, the pre-existing $s\bar{s}$ pairs in three nucleons can coalesce to form an Ω or $\bar{\Omega}$ during the collision. A combination of partial coalescence and pair-creation is also possible. This is characterized by the small $s\bar{s}$ component in the nucleon wavefunction, but it can be a competing mechanism if the amplitude is comparable to that of the creation of 3 $s\bar{s}$ pairs via gluons. Furthermore, due to the combinatorics, one expects that the yield due to the dissociation-recombination mechanism from the pre-existing sea pairs will grow with the number of participant nucleons relative to that of the pair-creation mechanism.

To conclude, we have learned that there are surprisingly large strangeness contents in the nucleon in various channels, such as in the axial ($\bar{s}\gamma_\mu\gamma_5s$) and scalar ($\bar{s}s$) matrix elements. It would be interesting to find out what role they play in the hyper-antihyperon productions in heavy-ion collisions.

References

- [1] D. H. Beck, talk at this conference.
- [2] D.T. Spayde *et al.*, SAMPLE collaboration, *Phys. Rev. Lett.* **84**, 1106 (2000).
- [3] CEBAF proposal #PR-91-017, D. H. Beck, spokesperson; CEBAF proposal #PR-91-010, J. M. Finn and P. A. Soude, spokespersons; CEBAF proposal #PR-91-004, E. J. Beise, spokesperson.
- [4] G. Hohler, *PiN Newslett.* **15**, 123 (1999); Marc Knecht, *ibid.*, 108 (1999).
- [5] E.W. Hughes and R. Voss, *Ann. Rev. Nucl. Part. Sci.* **49**, 303 (1999).
- [6] N. Mathur, S.J. Dong, K.F. Liu, L. Mankiewicz, and N.C. Mukhopadhyay, to appear in *Phys. Rev. D*, hep-ph/9912289.
- [7] T. Adams *et al.*, NuTeV Collaboration, hep-ex/9906038; V. Barone, C. Pascaud, and F. Zomer, hep-ph/0004268.
- [8] A. De Rújula, H. Georgi, and S. L. Glashow, *Phys. Rev.* **D12**, 147, 1975.
- [9] K. F. Liu, and C. W. Wong, *Phys. Rev.* **D17**, 2350 (1978); *Phys. Rev.* **D21**, 1350 (1980); K. F. Liu and C. W. Wong, *Phys. Rev.* **D28**, 170 (1983).
- [10] N. Isgur and G. Karl, *Phys. Rev.* **D18**, 4187 (1978); *ibid.*, **D19**, 2653 (1979).
- [11] A. Chodos, R. L. Jaffe, K. Johnson, C. B. Thron, and V. F. Weisskopf, *Phys. Rev.* **D9**, 3471 (1974); A. Chodos, R. L. Jaffe, K. Johnson, and C. B. Thron, *Phys. Rev.* **D10**, 2599 (1974).
- [12] L. Brekke and J. Rosner, *Comments Nucl. Part. Phys.* **A18**, 83 (1988).
- [13] L. G. Pondrom, *Phys. Rev.* **D53**, 5322 (1996).
- [14] See for example, F. E. Close, An Introduction to Quarks and Partons, Academic Press, 1979.
- [15] S. Ono, *Nucl. Phys.* **B107**, 522 (1976).
- [16] R. Koniuk and N. Isgur, *Phys. Rev.* **D21**, 1868 (1980).
- [17] J. F. Donoghue, E. Golowich, and B. R. Holstein, Dynamics of the Standard Model, Cambridge University Press, 1992.
- [18] S. Okubo, *Phys. Lett.* **B5**, 165 (1963); G. Zweig, CERN Reports 8419/TH412 (1964); I. Iizuka, *Prog. Theor. Phys. Suppl.* **37-38**, 21 (1966).
- [19] J. Ashman *et al.* (EMC), *Phys. Lett.* **B206**, 364 (1988).
- [20] K. Abe *et al.* (E143), *Phys. Rev. Lett.* **74**, 346 (1995).
- [21] D. Adams *et al.* (SMC), *Phys. Rev.* **D56**, 5330 (1997).
- [22] S.J. Dong, J.-F. Lagaë, and K.F. Liu, *Phys. Rev. Lett.* **75**, 2096 (1995).
- [23] M. Fukugita, Y. Kuramashi, M. Okawa, and A. Ukawa, *Phys. Rev. Lett.* **75**, 2092 (1995).
- [24] S. Güsken *et al.*, hep-lat/9901009.
- [25] *Lattice '99*, Proceedings of the International Symposium, Pisa, 1999, edited by M. Campostrini *et al.* (*Nucl. Phys. B (Proc. Suppl.)* **83-84**, 2000) is a recent survey of lattice gauge theories.
- [26] H. Neuberger, *Phys. Lett.* **B417**, 141 (1998); R. Narayanan and H. Neuberger, *Nucl. Phys.* **B443**, 305 (1995).
- [27] S.J. Dong, F.X. Lee, K.F. Liu, and Z.B. Zhang, hep-lat/0006004.
- [28] W. Lee and D. Weingarten, *Phys. Rev.* **D59**, 094508 (1999).
- [29] For a review, see H. Y. Cheng, *Int. J. Mod. Phys.* **A11**, 5109 (1996).
- [30] K.F. Liu, S.J. Dong, T. Draper, J.M. Wu, and W. Wilcox, *Phys. Rev.* **D49**, 4755 (1994).
- [31] K.F. Liu, *Phys. Rev.* **D62**, 074501 (2000).

- [32] K. F. Liu, S. J. Dong, T. Draper, D. Leinweber, J. Sloan, W. Wilcox, and R. M. Woloshyn, *Phys. Rev.* **D59**, 112001 (1999).
- [33] F.E. Close and R.G. Roberts, *Phys. Lett.***B316**, 165 (1993).
- [34] T.P. Cheng, *Phys. Rev.* **D13**, 2161 (1976); *ibid* **D38**, 2869 (1988).
- [35] J. Gasser, H. Leutwyler, and M.E. Sanio, *Phys. Lett.* **B253**, 252, 260 (1991).
- [36] J. Gasser and H. Leutwyler, *Phys. Rep.* **87**, 77 (1982); J. F. Donoghue and C. R. Nappi, *Phys. Lett.***B168**, 105 (1986).
- [37] M. Fukugita, Y. Kuramashi, M. Okawa, and A. Ukawa, *Phys. Rev.* **D51**, 5319 (1995).
- [38] S.J. Dong, J.-F. Lagaë, and K.F. Liu, *Phys. Rev.* **D54**, 5496 (1996).
- [39] S. Güsken *et. al.*, *Phys. Rev.***D59**, 054504 (1999).
- [40] L. Maiani *et al.*, *Nucl. Phys.***293**, 420 (1987).
- [41] M. Okawa, *Nucl. Phys.***B** (Proc. Suppl.) **47**, 160 (1996).
- [42] J. Gasser, *Ann. Phys. (NY)* **136**, 62 (1981).
- [43] B. Mueller *et al.*, SAMPLE Collaboration, *Phys. Rev. Lett.* **78**, 3824 (1997).
- [44] S. J. Dong, K. F. Liu, and A. G. Williams, *Phys. Rev.* **D58**, 074504 (1998).
- [45] N. Mathur, talk at Lattice 2000, Bangalore, India, Aug. 2000.
- [46] D.B. Leinweber, *Phys. Rev.* **D53**, 5115 (1996).
- [47] Talks given by D. Rohrich, R. Barton, R. A. Fini, and V. Manzari in this conference.
- [48] F. Antinori, *et al.*, WA97 collaboration, *Nucl. Phys.***A661**, 130c (1999); R. Lietava, *et al.*, WA97 collaboration, *J. Phys.* **B25**, 181 (1999); E. Andersen, *et al.*, WA97 collaboration, *Phys. Lett.***B449**, 401 (1999).
- [49] F. Sikler, *et al.*, NA49 collaboration, *Nucl. Phys.***A661**, 45c (1999).
- [50] J. Rafelski and B. Müller, *Phys. Rev. Lett.***48**, 1066 (1982).
- [51] P. Braun-Munzinger, I. Heppe, and J. Stachel, *Phys. Lett.***B465**, 15 (1999); S. Hamieh, K. Redlich, and A. Tounsi, hep-ph/0006024.
- [52] S.E. Vance and M. Gyulassy, *Phys. Rev. Lett.***83**, 1735 (1999).
- [53] A. Capella and C.A. Salgado, *Phys. Rev.***C60**, 054906 (1999).
- [54] M. Bleicher, W. Greiner, H. Stöcker, and N. Xu, hep-ph/0007215.